ISSN 1070-3284, Russian Journal of Coordination Chemistry, 2021, Vol. 47, No. 7, pp. 488–501. © Pleiades Publishing, Ltd., 2021.
Russian Text © The Author(s), 2021, published in Koordinatsionnaya Khimiya, 2021, Vol. 47, No. 7, pp. 439–452.

Noncovalent Interactions in the Architectures with Substituted Salicylaldehyde Semicarbazones

L. N. Cuba[a], E. C. Gorincioi[a], D. P. Dragancea[a], S. G. Shova[a], and P. N. Bourosh[a, b, *]

[a] *Institute of Chemistry, Chisinau, Republic of Moldova*

[b] *Institute of Applied Physics, Chisinau, Republic of Moldova*

**e-mail: bourosh.xray@phys.asm.md*

Received January 18, 2021; revised January 29, 2021; accepted February 2, 2021

Abstract—The X-ray diffraction study of three compounds containing 2,3-dihydroxybenzaldehyde semicarbazone (H_3L^1) or 2-hydroxy-3-methoxybenzaldehyde semicarbazone (H_2L^2) shows the formation of one organic salt with protonated triethylamine $[(C_2H_5)_3NH][H_2L^1]\cdot0.5(CH_3)_2CO$ (**I**) and two new coordination nickel(II) compounds with these two differently substituted semicarbazones of salicylaldehyde $[Ni(H_3L^1)(H_2L^1)](NO_3)\cdot2.5MeOH\cdot0.25H_2O$ (**II**) and $[Ni(H_2L^2)_2]Cl_2\cdot4H_2O$ (**III**) (CIF files CCDC nos. 2041894–2041896 (**I**–**III**)). The Ni(II) compounds are ionic and formed by the complex cations with the same metal to ligand ratio. The Ni(II) ion in these complex cations is characterized by a distorted octahedral coordination geometry formed by a set of donor atoms N_2O_4 of two ligands coordinated via the tridentate mode. In the monocharged complex cation of compound **II**, two coordinated ligands are not identical. One of them acts as the neutral chelating agent (H_3L^1), and the second ligand is deprotonated and involved as the monoanion $(H_2L^1)^-$. Both H_2L ligands are neutral in the complex cation of compound **III.** In the crystal, all the three compounds form supramolecular ensembles of diverse dimensionality and architecture, and their components are joined by weak interactions of different types.

Keywords: coordination compounds, semicarbazone, salicylaldehyde, noncovalent interactions, X-ray diffraction analysis

DOI: 10.1134/S1070328421070034

INTRODUCTION

Weak noncovalent contacts, such as hydrogen bond, π–π stacking, van der Waals interactions, and others, play a significant role in modern crystal engineering. These directed interactions can bind individual components, including crystallization molecules, into various associates, clusters, and supramolecular systems to form new functional materials [1, 2].

Transition metal complexes based on acylhydrazones as ligands form various supramolecular ensembles [3–5]. The use of semicarbazones for the synthesis of a broader variety of the complexes is caused not only by different denticities of the ligands and easy methods of their synthesis but by the interesting pharmacological properties of the ligands as well [6–8]. On the one hand, salicylaldehyde (2-hydroxybenzaldehyde) and its derivatives are also convenient carbonyl precursors for these systems, and the V(V), Cu(II), and Zn(II) complexes with semicarbazone are characterized by diverse fruitful properties [9–12]. On the other hand, interesting supramolecular crystalline architectures are often formed due to the proton of the amide N–H fragment, which is sensitive to hydrogen bond formation and similar to that in related hydrazones (R–C(=O)–NH–). The presence of appropriate additional functional groups (e.g, hydroxy or methoxy) can increase the denticity of the formed Schiff base and, as a consequence, can change the chelating ability and structural flexibility. Thus, some hydrazone ligands with a set of donor atoms N,O in the hydrazone fragment have various coordination modes to metal ions in the aldehyde moiety and also due to the presence of additional functional groups, which results in the formation of both mononuclear Ni(II) complexes [13], binuclear Mn(II) complexes [14–16], tetranuclear Cu(II) [17, 18], Co(II) [19], and Ni(II) clusters [20], and heterometallic potassium dioxidovanadium(IV) polymers [21].

Continuing the studies of the coordination ability of semicarbazones of various salicylaldehyde derivatives [22], we synthesized and structurally studied uncoordinated semicarbazone formed as the organic salt $[(C_2H_5)_3NH][H_2L^1]\cdot0.5(CH_3)_2CO$ (**I**) and two Ni(II) complexes, $[Ni(H_3L^1)(H_2L^1)](NO_3)\cdot2.5MeOH\cdot0.25H_2O$ (**II**) and $[Ni(H_2L^2)_2]Cl_2\cdot4H_2O$ (**III**), where H_3L^1 is 2,3-dihydroxybenzaldehyde semicarbazone, and H_2L^2 is 2-hydroxy-3-methoxybenzaldehyde semicarbazone.

EXPERIMENTAL

Commercial reagents and solvents (reagent grade) were used as received.

Synthesis of ligands. Ligands H_3L^1 and H_2L^2 were synthesized using the modified procedures described in [23] and [24], respectively. 2,3-Dihydroxybenzaldehyde (1.38 g, 10 mmol) or 2-hydroxy-3-methoxybenzaldehyde (1.52 g, 10 mmol) was added to a solution of hydrochloric semicarbazide (1.11 g, 10 mmol) and sodium acetate trihydrate (1.36 g, 10 mmol) in a water–ethanol (1 : 2 vol/vol) mixture (15 mL), and the resulting mixture was stirred at room temperature for 1 h. The formed suspension was filtered off, and the precipitate was washed with ethanol and dried in air. The yields were 81% for H_3L^1 and 93% for H_2L^1.

H_3L^1: IR (ν, cm^{-1}): 3600, 3483, 3454, 3436, 3346, 1669, 1592, 1279, 1221. ^1H NMR (δ, ppm): 6.37 (br.s., 2H, NH_2), 6.63 (t, J = 7.8 Hz, 1H, Ar–H^5), 6.75 (dd, J = 7.8 Hz, 1.5, 1H, Ar–H^4), 7.17 (d, J = 7.8 Hz, 1H, Ar–H^6), 8.13 (s, 1H; HC=N), 9.19, 9.41 (br.s, 2H, OH), 10.18 (br.s, 1H; CONH). ^{13}C NMR (δ, ppm): 115.84 (ArC_4), 117.30 (ArC_6), 118.96 (ArC_5), 120.96 (ArC_1), 138.55 (CH=N), 144.54 (ArC_2–OH), 145.43 (ArC_3–OH), 156.38 (C=O). ^{15}N NMR: 77 (NH_2), 154 (NH–CO), 313 (N=CH).

H_2L^2: IR (ν, cm^{-1}): 3465, 3329, 3267, 1672, 1585, 1264, 1218. ^1H NMR (δ, ppm): 3.80 (s, 3H, OCH_3), 6.40 (br.s, 2H, NH_2), 6.76 (d, J = 7.9 Hz, 1H, Ar–H^5), 6.91 (d, J = 7.9 Hz, 1H, Ar–H^4), 7.38 (d, J = 7.8 Hz, 1H, Ar–H^6), 8.16 (s, 1H; HC=N), 9.30 (br.s, 1H, OH), 10.21 (br.s, 1H; CONH). ^{13}C NMR (δ, ppm): 55.85 (ArC_3–OCH_3), 112.21 (ArC_4), 118.16 (ArC_6), 118.96 (ArC_5), 121.08 (ArC_1), 137.24 (CH=N), 145.32 (ArC_2–OH), 147.88 (ArC_3–OCH_3), 156.62 (C=O). ^{15}N NMR: 77 (NH_2), 155 (NH–CO), 315 (N=CH).

Synthesis of compound I. Triethylamine (Et_3N) (10 droplets) was added to a warm suspension containing H_3L^1 (0.05 g) in acetone (15 mL), and the gradual dissolution of the compound was observed. The obtained light yellow solution was left to stay at room temperature in a closed bottle in which the formation of transparent needle-like single crystals suitable for X-ray diffraction analysis (XRD) was observed on the same day. Evidently, acetone molecules of crystallization were lost rather easily upon the exposure of the crystals to atmosphere at the environmental temperature with an appreciable influence on the morphology of the crystal. Solvent losses were avaided for the XRD experiment.

^1H NMR (δ, ppm): 0.93 (t, 9H, J = 7.1 Hz, $N(CH_2CH_3)_3$), 2.08 (s, 6H, acetone), 2.43 (q, 6H, J = 7.1 Hz, $N(CH_2CH_3)_3$), 6.36 (br.s, 2H, NH_2), 6.62 (d, J = 7.8 Hz, 1H, Ar–H^5), 6.74 (d, J = 7.7 Hz, 1H, Ar–H^4), 7.17 (d, J = 7.8 Hz, 1H, Ar–H^6), 8.13 (s, 1H; HC=N), 10.15 (br.s, 1H, CONH). ^{13}C NMR (δ, ppm): 11.64 and 45.74 (triethylamine), 30.56 (acetone), 115.77 (ArC_4), 117.22 (ArC_6), 118.86 (ArC_5), 120.92 (ArC_1), 138.47 (CH=N), 144.57 (ArC_2–O), 145.44 (ArC_3–O), 156.32 (C=O), 206.29 (acetone). ^{15}N NMR: 47 (N^+), 77 (NH_2), 152 (NH–CO), 312 (N=CH).

Synthesis of compound II. A solution of $Ni(NO_3)_2 \cdot 6H_2O$ (0.146 g, 0.5 mmol) in methanol (10 mL) was poured dropwise to a suspension of H_3L^1 (0.098 g, 0.5 mmol) in methanol (20 mL) with permanent stirring. Then the mixture was heated in a water bath to the complete dissolution of semicarbazone, and the obtained light green solution was filtered through a paper filter. After some time, orthorhombic plates of light green single crystals suitable for XRD precipitated from the filtrate and were filtered off, washed with methanol, and dried in air. The yield was ~42%.

For $C_{18.5}H_{27.5}N_7O_{11.75}Ni$

Anal. calcd., %	C, 37.36	H, 4.66	N, 16.49
Found, %	C, 37.58	H, 4.88	N, 16.20

IR (ν, cm^{-1}): 3834, 3334, 3292, 1666, 1554, 1407, 1268, 1216, 577, 551, 489.

Synthesis of compound III. Ligand H_2L^2 (0.209 g, 1.0 mmol) was added to a hot solution of $NiCl_2 \cdot 6H_2O$ (0.238 g, 1.0 mmol) in ethanol (10 mL). The obtained mixture was heated to the boiling point for 30 min. Then the formed green solution was cooled at room temperature. After 3 days, a green crystalline precipitate containing single crystals suitable for XRD was filtered off, washed with diethyl ether, and dried at 120°C for 1.5 h. The yield was 0.152 g (49%).

For $C_{18}H_{22}N_6O_6Cl_2Ni$ (after water loss)

Anal. calcd., %	C, 39.45	H, 4.05	N, 15.36
Found, %	C, 39.27	H, 4.15	N, 15.18

IR (ν, cm^{-1}): 3465, 3329, 3284, 3223, 1663, 1590, 1536, 1253, 1230, 598, 584, 531, 471, 423.

The compositions and structures of the compounds were determined by elemental analysis, IR spectroscopy, and XRD analysis. IR spectra were recorded on a Perkin Elmer spectrum 100 FT-IR spectrometer in Nujol in ranges of 4000–400 and 4000–650 cm^{-1} (the latter for the attenuated total internal reflection (ATR) mode). High-resolution ^1H, ^{13}C, and ^{15}N NMR spectra were detected on an AVANCE III 400 MHz FT-IR NMR spectrometer (Bruker) with working frequencies of 400.13, 100.61, and 40.54 MHz, respectively. NMR experiments were carried out at 25°C. Dimethyl sulfoxide (DMSO-d_6, isotope enrichment 99.95%) served as the solvent. Chemical shifts (CS) (δ, ppm) refer to the residual sol-

Table 1. Crystallographic data and experimental structural characteristics for compounds **I**–**III**

Parameter	Value		
	I	**II**	**III**
Empirical formula	$C_{15.5}H_{27}N_4O_{3.5}$	$C_{18.50}H_{27.50}N_7O_{11.75}Ni$	$C_{18}H_{30}N_6O_{10}Cl_2Ni$
FW	325.41	594.68	620.09
Crystal system	Monoclinic	Monoclinic	Monoclinic
Space group	$C2/c$	$P2_1/c$	$C2/c$
a, Å	18.1901(17)	17.9605(11)	22.8033(11)
b, Å	14.0208(15)	12.8375(6)	10.7327(4)
c, Å	14.3246(12)	21.9246(13)	12.0921(4)
β, deg	92.716(8)	99.888(6)	117.447(3)
V, Å^3	3649.2(6)	4980.0(5)	2626.31(18)
Z	8	8	4
ρ_{calc}, g/cm^3	1.185	1.586	1.568
μ, mm^{-1}	0.085	0.854	1.004
F(000)	1408	2476	1288
Crystal sizes, mm	0.4 × 0.05 × 0.05	0.2 × 0.15 × 0.15	0.33 × 0.24 × 0.08
Range of θ, deg	2.91–25.05	1.85–25.50	3.16–25.50
Ranges of reflection indices	$-21 \le h \le 20$, $-16 \le k \le 16$, $-17 \le l \le 14$	$-21 \le h \le 20$ $-15 \le k \le 15$ $-17 \le l \le 26$	$-26 \le h \le 27$, $-12 \le k \le 12$, $-14 \le l \le 10$
Number of measured/ independent reflections (R_{int})	6255/3207 (0.0639)	23982/9260 (0.0593)	4848/2433 (0.0223)
Number of reflections with $I > 2\sigma(I)$	1242	6679	2036
Completeness, %	99.0	99.9	99.3
Number of refined parameters	233	715	172
GOOF	0.984	1.002	1.004
R_1, wR_2 ($I > 2\sigma(I)$)	0.0666, 0.0871	0.0679, 0.1389	0.0392, 0.1013
R_1, wR_2 (all data)	0.1790, 0.1194	0.1055, 0.1567	0.0509, 0.1091
$\Delta\rho_{max}/\Delta\rho_{min}$, e Å^{-3}	0.191/–0.193	0.578/–0.487	0.532/–0.275

vent peak (^{1}H: 2.50 ppm, ^{13}C: 39.50 ppm), and spin-spin coupling constant (J) are given in Hz. The 1D (^{1}H, ^{13}C) and 2D heteronuclear (^{1}H/^{13}C HSQC, ^{1}H/^{13}C HMBC, and ^{1}H/^{15}N HMQC, ^{1}H/^{15}N HMBC) NMR experiments were carried out using standard pulse sequences. The ^{15}N CS are presented with respect to liquid NH_3 [25]. The data were analyzed using the Bruker TOPSPIN 2.1 software.

XRD analyses for compounds **I**–**III** were carried out on Xcalibur E diffractometers (MoK_α radiation, λ = 0.71073 Å, graphite monochromator) at room temperature for compounds **I** and **III** and at 180 K for compound **II**. The experimental data were processed and the unit cell parameters were determined using the CrysAlis Oxford Diffraction Ltd. program [26]. The structures were solved by direct methods and refined by least squares mainly in the anisotropic full-matrix approximation for non-hydrogen atoms (SHELXS-97, SHELXL2014) [27, 28]. The crystallographic data and structural experimental characteristics for compounds **I**–**III** are presented in Table 1. Selected interatomic distances and bond angles are listed in Table 2. The geometric parameters of hydrogen bonds are given in Table 3.

The positional and thermal parameters for atoms of the studied compounds were deposited with the Cambridge Crystallographic Data Centre (CIF files CCDC nos. 2041894–2041896 (**I**–**III**); deposit@ccdc.cam.ac.uk or http://www.ccdc.cam.ac.uk/data_request/cif).

Table 2. Selected interatomic distances and bond angles in compounds **I**–**III**

Bond	*d*, Å	Bond	*d*, Å
		I	
C(2)–N(1)	1.282(3)	C(1)–O(1)	1.245(4)
N(1)–N(2)	1.386(3)	C(1)–N(3)	1.324(4)
N(2)–C(1)	1.359(4)		
		II	
Ni(1)–O(1*A*)	2.065(3)	Ni(2)–O(1*B*)	2.080(3)
Ni(1)–O(2*A*)	2.051(3)	Ni(2)–O(2*B*)	2.078(3)
Ni(1)–N(1*A*)	2.001(4)	Ni(2)–N(1*B*)	2.001(4)
Ni(1)–O(4*A*)	2.123(3)	Ni(2)–O(4*B*)	2.077(3)
Ni(1)–O(5*A*)	2.053(3)	Ni(2)–O(5*B*)	2.026(3)
Ni(1)–N(4*A*)	1.996(4)	Ni(2)–N(4*B*)	1.994(4)
C(2*A*)–N(1*A*)	1.288(6)	C(2*B*)–N(1*B*)	1.277(5)
N(1*A*)–N(2*A*)	1.379(5)	N(1*B*)–N(2*B*)	1.379(5)
N(2*A*)–C(1*A*)	1.361(6)	N(2*B*)–C(1*B*)	1.350(5)
C(1*A*)–O(1*A*)	1.246(5)	C(1*B*)–O(1*B*)	1.251(5)
C(1*A*)–N(3*A*)	1.319(6)	C(1*B*)–N(3*B*)	1.325(6)
C(10*A*)–N(4*A*)	1.280(6)	C(10*B*)–N(4*B*)	1.291(5)
N(4*A*)–N(5*A*)	1.379(5)	N(4*B*)–N(5*B*)	1.371(5)
N(5*A*)–C(9*A*)	1.364(6)	N(5*B*)–C(9*B*)	1.358(6)
C(9*A*)–O(4*A*)	1.257(5)	C(9*B*)–O(4*B*)	1.247(5)
C(9*A*)–N(6*A*)	1.319(6)	C(9*B*)–N(6*B*)	1.325(6)
		III	
Ni(1)–O(1)	2.045(2)	N(1)–N(2)	1.380(3)
Ni(1)–O(2)	2.048(2)	N(2)–C(1)	1.363(3)
Ni(1)–N(1)	2.006(2)	C(1)–O(1)	1.247(3)
C(2)–N(1)	1.273(3)	C(1)–N(3)	1.322(4)
Angle	ω, deg	Angle	ω, deg
		I	
C(2)N(1)N(2)	114.5(3)	N(2)C(1)O(1)	118.9(3)
N(1)N(2)C(1)	121.5(3)	O(1)C(1)N(3)	122.7(3)
N(2)C(1)N(3)	118.4(3)		
		II	
O(1*A*)Ni(1)O(2*A*)	167.21(12)	O(1*B*)Ni(2)O(2*B*)	165.31(12)
O(1*A*)Ni(1)N(1*A*)	78.92(14)	O(1*B*)Ni(2)N(1*B*)	79.68(13)
O(1*A*)Ni(1)O(4*A*)	94.29(13)	O(1*B*)Ni(2)O(4*B*)	96.63(12)
O(1*A*)Ni(1)O(5*A*)	91.97(13)	O(1*B*)Ni(2)O(5*B*)	88.14(12)
O(1*A*)Ni(1)N(4*A*)	93.07(13)	O(1*B*)Ni(2)N(4*B*)	94.37(13)
O(2*A*)Ni(1)N(1*A*)	88.29(14)	O(2*B*)Ni(2)N(1*B*)	86.79(13)
O(2*A*)Ni(1)O(4*A*)	87.29(12)	O(2*B*)Ni(2)O(4*B*)	89.51(12)
O(2*A*)Ni(1)O(5*A*)	89.47(12)	O(2*B*)Ni(2)O(5*B*)	88.92(12)
O(2*A*)Ni(1)N(4*A*)	99.68(13)	O(2*B*)Ni(2)N(4*B*)	99.94(13)
N(1*A*)Ni(1)O(4*A*)	98.08(14)	N(1*B*)Ni(2)O(4*B*)	92.12(13)
N(1*A*)Ni(1)O(5*A*)	95.87(14)	N(1*B*)Ni(2)O(5*B*)	101.26(13)
N(1*A*)Ni(1)N(4*A*)	171.17(15)	N(1*B*)Ni(2)N(4*B*)	168.35(15)
O(4*A*)Ni(1)O(5*A*)	165.57(12)	O(4*B*)Ni(2)O(5*B*)	166.41(12)

Table 2. (Contd.)

Angle	ω, deg	Angle	ω, deg
O(4*A*)Ni(1)N(4*A*)	78.64(14)	O(4*B*)Ni(2)N(4*B*)	78.54(14)
O(5*A*)Ni(1)N(4*A*)	88.06(14)	O(5*B*)Ni(2)N(4*B*)	88.45(14)
C(2*A*)N(1*A*)N(2*A*)	118.0(4)	C(2*B*)N(1*B*)N(2*B*)	117.9(4)
N(1*A*)N(2*A*)C(1*A*)	115.6(4)	N(1*B*)N(2*B*)C(1*B*)	116.1(4)
N(2*A*)C(1*A*)N(3*A*)	117.0(4)	N(2*B*)C(1*B*)N(3*B*)	115.5(4)
N(2*A*)C(1*A*)O(1*A*)	120.0(4)	N(2*B*)C(1*B*)O(1*B*)	121.4(4)
O(1*A*)C(1*A*)N(3*A*)	123.1(4)	O(1*B*)C(1*B*)N(3*B*)	123.0(4)
C(10*A*)N(4*A*)N(5*A*)	117.2(4)	C(10*B*)N(4*B*)N(5*B*)	118.4(4)
N(4*A*)N(5*A*)C(9*A*)	116.8(4)	N(4*B*)N(5*B*)C(9*B*)	115.4(4)
N(5*A*)C(9*A*)N(6*A*)	117.2(4)	N(5*B*)C(9*B*)N(6*B*)	116.7(4)
N(5*A*)C(9*A*)O(4*A*)	119.7(5)	N(5*B*)C(9*B*)O(4*B*)	120.1(4)
O(4*A*)C(9*A*)N(6*A*)	123.1(5)	O(4*B*)C(9*B*)N(6*B*)	123.1(4)
	III		
O(1)Ni(1)O(1)$^{\#1}$	93.37(11)	O(2)Ni(1)O(2)$^{\#1}$	87.70(12)
O(1)Ni(1)O(2)	166.79(7)	O(2)Ni(1)N(1)	87.58(8)
O(1)Ni(1)O(2)$^{\#1}$	90.91(8)	O(2)Ni(1)N(1)$^{\#1}$	95.63(8)
O(1)Ni(1)N(1)	79.48(8)	N(1)Ni(1)O(1)$^{\#1}$	97.44(7)
O(1)Ni(1)N(1)$^{\#1}$	97.44(7)	N(1)Ni(1)N(1)$^{\#1}$	175.56(12)
C(2)N(1)N(2)	118.0(2)	N(2)C(1)O(1)	119.9(2)
N(1)N(2)C(1)	115.5(2)	O(1)C(1)N(3)	122.6(3)
N(2)C(1)N(3)	117.5(2)		

Symmetry codes: $^{\#1}$ $-x + 1, y, -z + 1/2$ (**III**).

RESULTS AND DISCUSSION

Ligands H_3L^1 and H_2L^2 were synthesized by the condensation of semicarbazide with 2,3-dihydroxybenzaldehyde and 2-hydroxy-3-methoxybenzaldehyde, respectively (Scheme 1). The structures of the synthesized ligands were confirmed by IR and NMR spectroscopy.

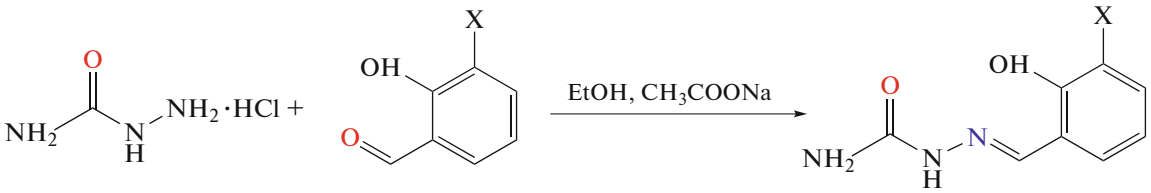

X = OH, H_3L^1

X = OCH_3, H_2L^2

Scheme 1.

The ^{1}H NMR spectral characteristics of ligand H_3L^1 obtained for solutions in DMSO-d_6 and MeOD-d_4 were described [23]. The ^{1}H CS of ligand H_3L^1 detected by us in a DMSO-d_6 solution coincide with the published data [23] and supplement them. For example, the signals of the aryl protons H^4–H^6 (cross peaks at 6.75/115.84, 6.63/118.96, and 7.17/117.30, respectively) were exactly assigned using the heteronuclear ^{1}H/^{13}C HSQC experiment. The CS of the carbon and nitrogen nuclei in ligand H_3L^1 obtained using ^{1}H/^{13}C HSQC, ^{1}H/^{13}C HMBC, ^{1}H/^{15}N HMQC, and ^{1}H/^{15}N HMBC experiments are presented for the first time. The methine carbon of the CH=N fragment in the ^{1}H/^{13}C HSQC spectrum is determined by the cross

Table 3. Geometric parameters of hydrogen bonds in compounds **I**–**III**

Contact D–H···A	Distance, Å			Angle DHA, deg	Coordinates of atoms A
	D–H	H···A	D···A		
			I		
N(4)–H(1)···O(2)	0.98	1.68	2.661(4)	177	x, y, z
N(3)–H(1)···O(2)	0.86	2.30	3.008(4)	140	$x, -y, z + 1/2$
N(3)–H(2)···O(1)	0.86	2.08	2.928(3)	171	$-x + 1, y, -z + 3/2$
N(2)–H(1)···O(1)	0.86	2.01	2.848(4)	166	$-x + 1, -y, -z + 1$
O(3)–H(1)···O(2)	0.82	2.17	2.641(3)	117	x, y, z
			II		
N(2*A*)–H(1)···O(3)	0.86	2.06	2.829(5)	149	$x, -y + 1/2, z - 1/2$
N(2*A*)–H(1)···O(1)	0.86	2.55	3.278(6)	144	$x, -y + 1/2, z - 1/2$
N(3*A*)–H(1)···O(1*B*)	0.86	2.53	3.332(5)	156	$x, -y + 3/2, z - 1/2$
N(3*A*)–H(2)···O(1)	0.86	2.23	3.057(6)	161	$x, -y + 1/2, z - 1/2$
N(5*A*)–H(1)···O(8)	0.86	2.01	2.839(5)	162	$-x + 1, -y + 2, -z + 1$
N(6*A*)–H(1)···O(4)	0.86	2.09	2.938(5)	170	$-x + 1, -y + 1, -z + 1$
N(6*A*)–H(1)···O(5)	0.86	2.72	3.233(6)	120	$-x + 1, -y + 1, -z + 1$
N(2*B*)–H(2)···O(4)	0.86	2.02	2.876(5)	178	x, y, z
N(3*B*)–H(1)···O(1*A*)	0.86	2.04	2.851(5)	157	$x, -y + 3/2, z + 1/2$
N(3*B*)–H(2)···O(6)	0.86	2.04	2.879(6)	164	x, y, z
N(5*B*)–H(1)···O(9)	0.86	1.84	2.671(6)	161	$x - 1, y, z$
N(6*B*)–H(1)···O(4*B*)	0.86	2.13	2.936(5)	155	$x, -y + 1, -z + 1$
N(6*B*)–H(2)···O(2)	0.86	2.22	2.958(6)	145	$x, -y + 1, -z + 1$
O(2*A*)–H(1)···O(5*B*)	0.63	1.84	2.459(4)	165	x, y, z
O(3*A*)–H(1)···O(7)	0.82	1.88	2.691(5)	171	x, y, z
O(6*A*)–H(1)···O(10)	0.82	1.78	2.599(5)	174	$x - 1, y, z$
O(2*B*)–H(1)···O(5*A*)	0.89	1.62	2.487(4)	166	x, y, z
O(3*B*)–H(1)···O(6*A*)	0.82	1.88	2.648(5)	157	x, y, z
O(6*B*)–H(1)···O(3*A*)	0.82	2.01	2.801(5)	163	x, y, z
O(7)–H(1)···O(4*A*)	0.82	2.07	2.875(5)	165	$-x + 1, -y + 1, -z + 1$
O(8)–H(1)···O(5)	0.82	2.19	2.937(6)	151	$-x + 1, y + 1/2, -z + 3/2$
O(8)–H(1)···O(6)	0.82	2.43	3.091(6)	139	$-x + 1, y + 1/2, -z + 3/2$
O(9)–H(1)···O(1*w*)	0.88	1.70	2.54(7)	159	$-x + 1, -y + 2, -z + 1$
O(9)–H(1)···O(11)	0.88	1.85	2.67(7)	155	$-x + 1, -y + 2, -z + 1$
O(10)–H(1)···O(2)	0.82	1.99	2.786(6)	162	$-x + 1, -y + 1, -z + 1$
O(11)–H(1)···O(3*B*)	0.94	1.90	2.83(7)	178	$x, -y + 3/2, z + 1/2$
O(12)–H(1)···O(1*B*)	0.92	1.97	2.888(12)	177	x, y, z
O(1*w*)–H(1)···O(3*B*)	0.85	1.99	2.83(7)	176	$x, -y + 3/2, z + 1/2$
O(1*w*)–H(2)···O(12)	0.80	1.89	2.69(4)	177	x, y, z
			III		
N(3)–H(1)···O(2*w*)	0.86	2.23	3.000(4)	149	x, y, z
N(3)–H(2)···Cl(1)	0.86	2.48	3.295(3)	158	x, y, z
N(2)–H(1)···Cl(1)	0.86	2.73	3.453(2)	142	x, y, z
O(2)–H(1)···O(1*w*)	0.82	1.86	2.573(3)	146	x, y, z
O(1*w*)–H(1)···Cl(1)	0.85	2.31	3.146(2)	167	$-x + 1, -y + 2, -z$
O(1*w*)–H(2)···Cl(1)	0.85	2.40	3.200(2)	158	$x-1/2, y - 1/2, z$
O(2*w*)–H(1)···Cl(1)	0.85	2.35	3.200(3)	173	$x, -y + 2, z + 1/2$
O(2*w*)–H(2)···Cl(1)	0.85	2.50	3.326(3)	166	$-x + 3/2, -y + 5/2, -z + 1$

peak at 8.13/138.55 ppm, whereas the long-range C–H correlation of the same proton with the carbon atoms at 120.96, 117.30, and 144.54 ppm in the $^{1}H/^{13}C$ HMBC spectrum made it possible to correctly determine the CS of the aryl carbon atoms C_1, C_6, and C_2, respectively (Scheme 2). Some key heterocorrelations $^{1}H/^{13}C$ HMBC, $^{1}H/^{15}N$ HMQC, and $^{1}H/^{15}N$ HMBC for determining the ^{13}C and ^{15}N NMR characteristics of ligand H_3L^1 are shown in Scheme 2.

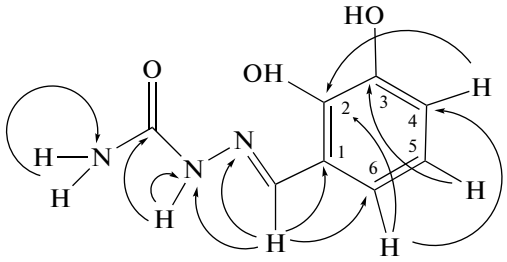

Scheme 2.

The data of the NMR spectra for H_2L^2 were published [29–31]. A comparative analysis of the data from these sources proved the doubtless advantage of 2D HETCOR NMR experiments for the exact determination of the CS of magnetically active nuclei. For example, only the ^{1}H NMR characteristic of ligand H_2L^2 exactly coinciding with our value was found using the $^{1}H/^{13}C$ heterocorrelation technique [30]. However, we found some distinctions in the CS assignment in the description of the ^{1}H and ^{13}C NMR spectral data [24, 29] and can explain them by the absence of the 2D HETCOR NMR technique among the methods used. For instance, the CS of the amide proton of the C(=O)–NH fragment (8.17 ppm in [29], our data are 10.21 ppm) was attributed to the methine N=CH (10.25 ppm in [29], our data are 8.16 ppm). The nucleus of methine carbon N=CH is described [29] by the CS at 147.88 ppm, and the following CS of the aryl nuclei C_1–C_3 and C_6 were described: 118.13, 137.21, 145.31, and 121.09 ppm, respectively. Our 2D HETCOR NMR experiments with the H_2L^2 sample completely prove the validity of the CS assignment of the studied ^{1}H, ^{13}C, and ^{15}N nuclei. The resolution of the amide and methine protons in the C(=O)–NH and N=CH fragments disappeared after the $^{1}H/^{15}N$ HMQC and $^{1}H/^{13}C$ HSQC experiments were performed: distinct cross peaks at 10.21/155 and 8.16/137.24 ppm were observed in the corresponding spectra. These results allowed us (1) to determine the following CS of the protonated nitrogen nuclei for the first time: amine nitrogen at 77 ppm (cross peak at 6.40/77 ppm in the $^{1}H/^{15}N$ HMQC spectrum) and amide nitrogen at 155 ppm (cross peak at 10.21/155 ppm in the $^{1}H/^{15}N$ HMQC spectrum) and (2) to characterize the methine carbon of N=CH by the CS at 137.24 ppm (cross peak at 8.16/137.24 ppm in the $^{1}H/^{13}C$ HSQC spectrum) differed from the value of CS at 147.88 ppm [28]. The CS of the aryl nuclei C_1–C_3 and C_6 were refined from the $^{1}H/^{13}C$ HMBC experiments. Some selected $^{1}H/^{13}C$ HMBC and $^{1}H/^{15}N$ HMBC correlations for the determination of the ^{13}C and ^{15}N NMR characteristics of ligand H_2L^2 are shown in Scheme 3.

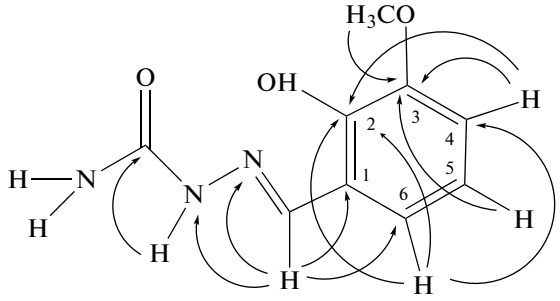

Scheme 3.

Thus, the experimental $^{1}H/^{13}C$ and $^{1}H/^{15}N$ NMR heterocorrelation techniques multiply proved their significance for the exact interpretation of the spectral data, and they are irreplaceable for the precise assignment of NMR signals in the spectrum. If some circumstances do not allow signal assignment, then it seems reasonable to list the corresponding values of CS.

The ^{1}H NMR spectrum of organic salt **I** contains all signals from the protons of ligand H_3L^1 except for the hydroxyl protons. A very broad signal at 0.15 ppm corresponding to the amide proton in ligand H_3L^1 only includes, most likely, the cationic proton of triethylamine and the proton of the hydroxyl group at ArC_3 in addition to the amide proton. This is confirmed, in turn, by the characteristic shape of this signal proving the presence of the hydrogen bond involving the cationic and hydroxyl protons. Thus, the presence of the hydrogen bond was also proved in a DMSO-d_6 solution. A comparative analysis of the CS of the protons of the H_3L^1 fragment in salt **I** and in the free ligand showed no substantial differences. The presence of both the triethylamine fragment and crystallization acetone in compound **I** was proved by the signals at 0.93, 2.43, and 2.08 ppm, respectively. The 1D and 2D heterocorrelation experiments for compound **I** gave the ^{13}C, ^{15}N, $^{1}H/^{13}C$ HSQC, $^{1}H/^{13}C$ HMBC, $^{1}H/^{15}N$ HMQC, and $^{1}H/^{15}N$ HMBC spectral data that completely confirmed the structure of the compound. The resonance frequencies of the ^{13}C and ^{15}N nuclei in salt **I** remain nearly unchanged compared to those in H_3L^1, whereas the signals of triethylamine (11.64 and 45.74 ppm) and acetone (30.56 and 206.29 ppm) were additionally detected. The nitrogen nuclei of protonated Et_3N were determined by the $^{1}H/^{15}N$ HMBC experiment: the protons of the methyl group of triethylamine at 0.93 ppm showed the long-range N–H correlation with nitrogen at 47 ppm, whereas the het-

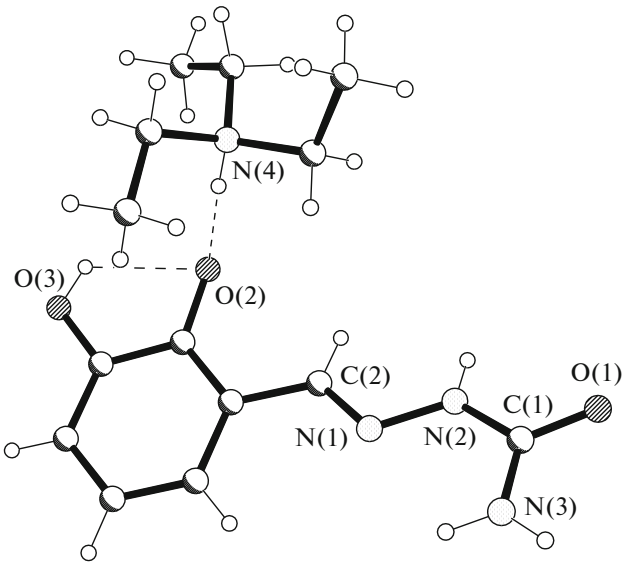

Fig. 1. Structures of the organic cation and anion in compound **I** with the partial notation of the atoms.

eronuclear multiple-bonded correlations of $^{1}H/^{15}N$ with the azomethine proton at 8.13 ppm were detected for the azomethine (312 ppm) and amide (152 ppm) nitrogen nuclei. The $^{1}H/^{15}N$ HMQC heterocorrelation made it possible to unmistakenly determine nitrogen of the amino group (two protons resonating at 6.36 ppm correlate with nitrogen at 77 ppm).

The IR spectrum of ligand H_3L^1 (in Nujol) exhibits broad bands at ~3600 and ~3483 cm^{-1} (sh) corresponding to ν(O–H) of water and associated phenol –OH groups in the ortho and meta positions; two medium-intensity bands at 3454 and 3436 cm^{-1} corresponding to the ν_{as} and ν_s(N–H) stretching vibrations, respectively, in the $-NH_2$ group; the weak ν(N–H) band of secondary amine at 3346 cm^{-1}; the strong ν(C=O) band of amide **I** at 1695 cm^{-1}; the medium ν(C=N) + δ(N–H) band of amide **II** at 1669 cm^{-1}; the ν(C=N) band at 1592 cm^{-1}; and the medium ν(C–O(phenol)) broad band at 1279 cm^{-1} along with the weak one at 1221 cm^{-1}.

The IR spectrum of ligand H_2L^2 (in Nujol) exhibits a strong narrow absorption band ν(N–H) at 3465 cm^{-1} and that of secondary amine at 3329 cm^{-1}; possibly, the ν(O–H) band of the phenol group in the ortho position at 3267 cm^{-1}; the strong ν(C=O) band of amide **I** at 1672 cm^{-1}; the strong ν(C=N) band at 1585 cm^{-1}; and the strong broad $\nu(C-O_{phenol})$ band at 1264 cm^{-1}.

A comparative analysis of the IR spectra of the ligands and complexes **II** and **III** showed that the broad bands (as shoulders) remained at ~3600–3400 cm^{-1}, indicating the presence of intermolecular hydrogen bonds between the associated O–H groups of the solvent molecules and phenol groups. The ν_{as} and ν_s(N–H) stretching vibration bands of the NH_2 group appear at 3334 (**II**) and 3465 (**III**) cm^{-1}, i.e., the shift to the low-frequency range due to the participation in hydrogen bond formation. The medium broad ν(N–H) band of secondary amine observed in the spectrum of the complexes at 3292 (**II**) and 3329 (**III**) cm^{-1}, respectively, almost does not change its position (shift by ~10 cm^{-1}). The strong bands ν(C=O) of amide **I** and ν(C=N) shift to the low-frequency range by 29 and 38 cm^{-1} (**II**) and by 10 and 46 cm^{-1} (**III**), respectively, due to the coordination of the carbonyl oxygen atom and azomethine nitrogen atom to the nickel(II) atom. The following new absorption bands appear: ν(Ni–O) at 577 and 551 cm^{-1}, ν(Ni–N) at 489 cm^{-1} (**II**), ν(Ni–O) at 598, 584, and 551 cm^{-1}, and ν(Ni–N) at 471 and 423 cm^{-1} (**III**). The medium-intensity ν(C–OH) absorption band in the spectrum bifurcates into absorption bands at 1268 and 1216 cm^{-1} (**II**), which indicates the possible presence of both nondeprotonated and deprotonated phenol groups. The presence of the strong broadened band at 1407–1332 cm^{-1} in the ATR spectrum of complex **II** corresponds, most likely, to the ν_3(NO) absorption band of the free nitrate ion.

The single crystals of salt $[(C_2H_5)_3NH][H_2L^1]\cdot 0.5(CH_3)_2CO$ (**I**) suitable for XRD were obtained from acetone in the presence of triethylamine when the solubility of the ligand in various polar solvents was studied. Compound **I** of the ionic type crystallizes in the monoclinic space group *C*2/*c* (Table 1) and contains both the cation of protonated triethylamine and the anion: semicarbazone with the deprotonated hydroxyl group in the ortho position and the acetone molecule disordered over two positions. The structure of compound **I** is presented in Fig. 1.

The conformation of the organic cation in compound **I** can be described by the positions of two groups (phenyl ring and semicarbazone group) relative to the C=N and N–C bonds in the semicarbazone fragment C(2)=N(1)–N(2)–C(1)(=O(1))–N(3), respectively (notation of the atoms corresponds to the notation of the atoms in the structure). The conformations of semicarbazones are shown in Scheme 4. An analysis of the general structural properties of the semicarbazone molecule [31–33] shows that the O(1) atom usually exists in the anti position relative to the hydrazine N(1) atom (Scheme 4b). The hydroxyl group of the phenyl ring can also exist in different positions relative to the C(2)=N(1) azomethine bond (Scheme 4c) [24, 34].

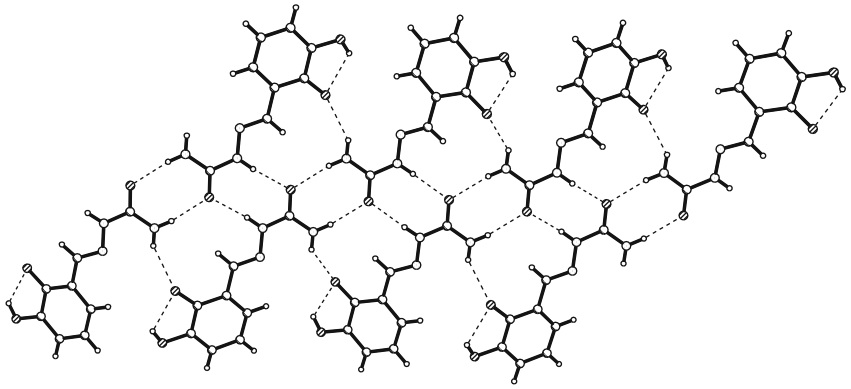

Fig. 2. Formation of chains of the anions in compound **I**.

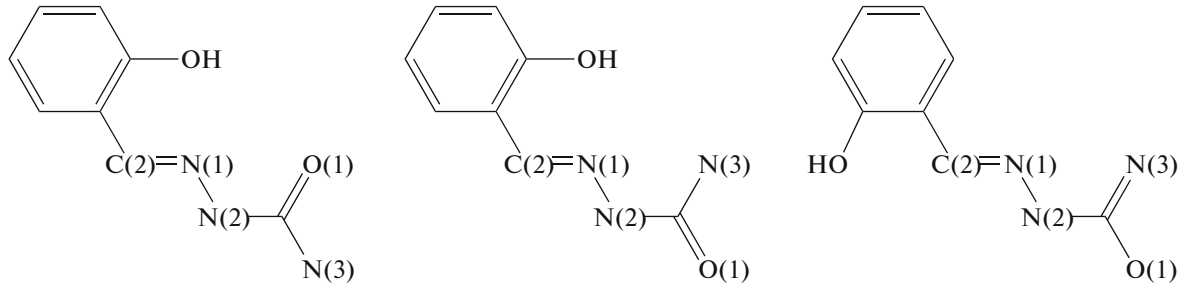

Scheme 4.

The structure of the semicarbazone anion in compound **I** indicates its stabilization in the anti conformation but with the rotation of the hydroxyl groups by 180° around the C–C(2) bond (Scheme 4c, Fig. 1). Upon complex formation this ligand can easily rotate around two ordinary bonds C(1)–N(2) and C(2)–C by 180° in such a way that all the three donor atoms would be in the position suitable for coordination (Scheme 4a). This indicates a high flexibility of these Schiff bases and the importance of intra- and intermolecular interactions in the determination of their configurations. The N(1)–N(2), N(2)–C(1), C(1)–N(3), and C(1)–O(1) bonds in compound **I** (Table 2) have the character of partial double bond, which indicates the electron density delocalization in the semicarbazone fragment, and are comparable with similar bonds in the semicarbazone derivatives of the aromatic carbonyl compounds [31–33].

The components in the crystal of compound **I** are bound to each other via the system of hydrogen bonds (Table 3) to stabilize the semicarbazone configuration, since the hydroxyl bond in the latter is involved in the intramolecular hydrogen bond in which the oxygen atom of the adjacent deprotonated OH groups serves as the acceptor, i.e., the oxygen atom in the ortho position. The carbonyl and alternating terminal/non-terminal amino groups of the adjacent anions are joined into synthones $R_2^2(8)$ via the hydrogen bonds N–H···O and O–H···O to form chains additionally stabilized by the N–H···O hydrogen bonds (Fig. 2), where the oxygen atom in the ortho position acts as the acceptor. The same oxygen atom is involved as the acceptor in the intermolecular hydrogen bond N–H···O, which binds the organic cations and anions/chains of the anions (Figs. 1, 3). The acetone molecules of crystallization are bound to the cations by the intermolecular hydrogen bonds C–H···O (C···O 3.242 Å, H···O 2.315 Å, angle CHO 160°) in which the oxygen atom of acetone is the acceptor.

Compound **II** was synthesized by the reaction of H_3L^1 with Ni(II) nitrate in methanol. Under the same conditions, the use of H_3L^2 and Ni(II) chloride resulted in the formation of compound **III**. Compounds **II** and **III** are ionic and consist of monomeric complex cations $[Ni(H_2L^1)(HL^1)]^+$ and anions $(NO_3)^-$ or of cations $[Ni(H_2L^2)_2]^{2+}$ and anions Cl^-, respectively. The crystals of these compounds also involve various solvate molecules. The coordination polyhedron of the Ni(II) ion in compounds **II** and **III** is a distorted octahedron, since two tridentate organic ligands coordinate in either the neutral or mono-

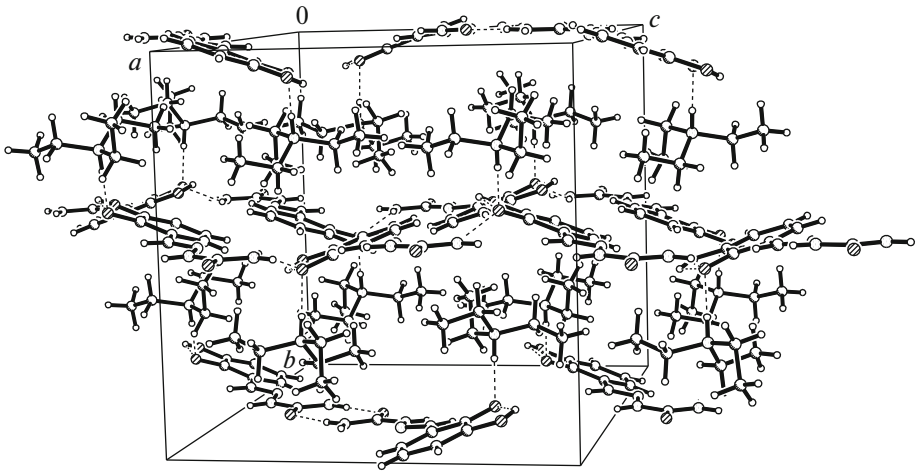

Fig. 3. Packing fragment of structural units in the crystal of compound **I**.

deprotonated form and uses the same set of ONO donor atoms: the carbazide and phenol oxygen atoms and the azomethine nitrogen atom (Fig. 4). Thus, in compound **II** both ligands retain the coordination mode and differ by the degree of deprotonation: one of them is coordinated as a monodeprotonated ligand, and the second ligand is coordinated as a neutral ligand, whereas in compound **III** both ligands are involved in coordination in the neutral form. It should be mentioned that this behavior of the tridentate ONO Schiff base in the bis(chelated) Ni(II) complex is unusual and rarely met as in compound **II** [13]. In the coordination polyhedra of Ni(II) in compounds **II** and **III**, the equatorial plane is formed by the ONO atoms of one tridentate ligand and one nitrogen atom of another ligand, whereas other two oxygen atoms of the second ligand are arranged at the vertices (Fig. 4). Two conjugated metallocycles are formed due to the coordination of these organic ligands to the metal atoms: five-membered semicarbazide metallocycle and six-membered salicylaldehyde metallocycle. The bond lengths and bond angles in the coordination polyhedra of the Ni(II) ions in compounds **II** and **III** are close to similar values in the octahedral complexes of this metal with tridentate thio- and semicarbazones of salicylaldehyde [35, 36]. The bond lengths in the organic ligands of these compounds differ slightly (Table 2), but their values confirm the stabilization of the latter in the keto form.

Compound $[Ni(H_2L^1)(HL^1)](NO_3)\cdot 2.5MeOH\cdot 0.25H_2O$ (**II**) crystallizes in the monoclinic space group $P2_1/n$ (Table 1). The independent part of the unit cell contains two crystallographically independent Ni(II) complexes **A** and **B**. The structure of complex **A** with the partial notation of atoms is shown in Fig. 4a, and the notation in complex **B** is similar. The components in the crystal are joined by a complicated system of hydrogen bonds, since the complex cations contain several OH and NH groups involved as proton donors, and the oxygen atoms O(1)–O(6) of the outer-sphere $(NO_3)^-$ anions participate as acceptors (Table 3, Fig. 5). The chains of complex cations **A** and **B** are observed in the crystal. They are associated into dimers via the intermolecular hydrogen bonds O–H···O involving the phenol oxygen atoms (Fig. 6), and the latter develop further using the intermolecular hydrogen bonds N–H···O between the amino groups and the oxygen atom of the carbonyl group. This arrangement favors the formation of π–π-stacking interactions between similar aromatic rings of complexes **A** and **B**, and the interplane average distance between them is 3.632 and 3.717 Å, respectively. The supramolecular architecture of the crystal is formed due to strong intermolecular hydrogen bonds in which the methanol and water molecules of crystallization are also involved to form intermolecular hydrogen bonds N–H···O, O–H···O, O(*w*)–H···O, and O–H···O(*w*) (O(7)–O(12) are the oxygen atoms of the methanol molecules) (Table 3). As a result, the complex cations and outer-sphere anions are joined between each other and via crystallization molecules. Weak intermolecular hydrogen bonds between both the cations and anions (e.g., C···O(5) (x, $-y + 1/2$, $z - 1/2$) 3.386 Å, H···O 2.63 Å, angle CHO 139°) and the methanol molecules and anions (C···O(1) ($-x + 1$, $-y + 1$, $-z + 1$) 3.370 Å, H···O 2.49 Å, angle CHO 152°) were additionally revealed in the crystal.

Compound $[Ni(H_2L^2)_2]Cl_2\cdot 4H_2O$ (**III**) crystallizes in the monoclinic space group $C2/c$ (Table 1). The independent part of the unit cell of this crystal contains half a centrosymmetric complex cation $[Ni(H_2L^1)_2]^{2+}$ (Fig. 4b), one outer-sphere anion Cl^-, and two water molecules of crystallization. The functional methoxy group of organic neutral ligand H_2L^2

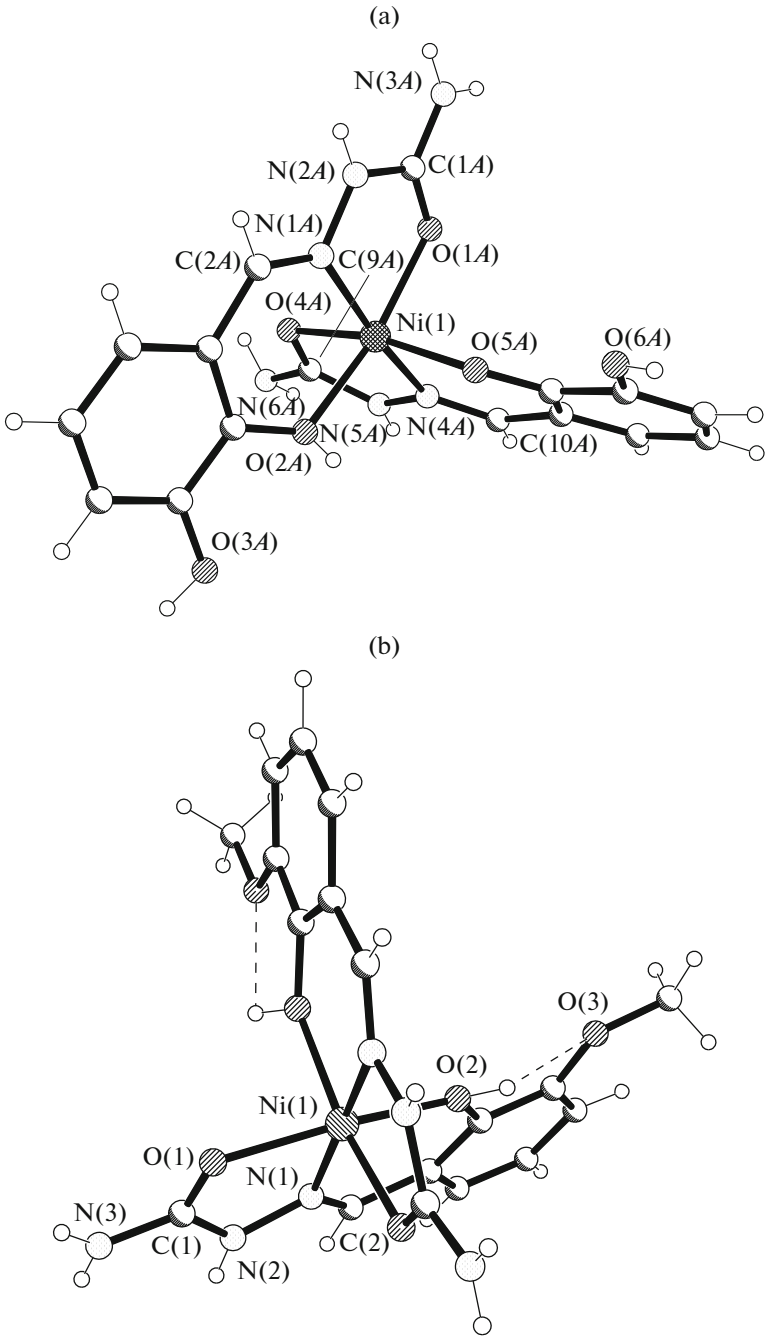

Fig. 4. Structures of (a) complex cation A in compound **II** and (b) complex cation in compound **III** (partial notation).

does not participate in coordination with the metal ion but its oxygen atom is involved as an acceptor in the formation of the intramolecular hydrogen bond O–H···O. The components of the crystal of compound **III** are joined by a system of intermolecular hydrogen bonds in which all OH and NH groups of the complex cations act as proton donors and Cl^- anions and oxygen atoms of water molecules of crystallization act as acceptors, and the latter are involved as both donors and acceptors (Fig. 7): the complex cations are bound to the Cl^- anions as both hydrogen bonds N–H···Cl and via hydrogen bonds of the water molecules O–H···O(*w*), N–H···O(*w*), and O(*w*)–H···Cl (Table 3). The system of intermolecular hydrogen bonds involves the methyl groups of the methoxy and C(2)–H fragments as donors and the O(1) atoms of the organic

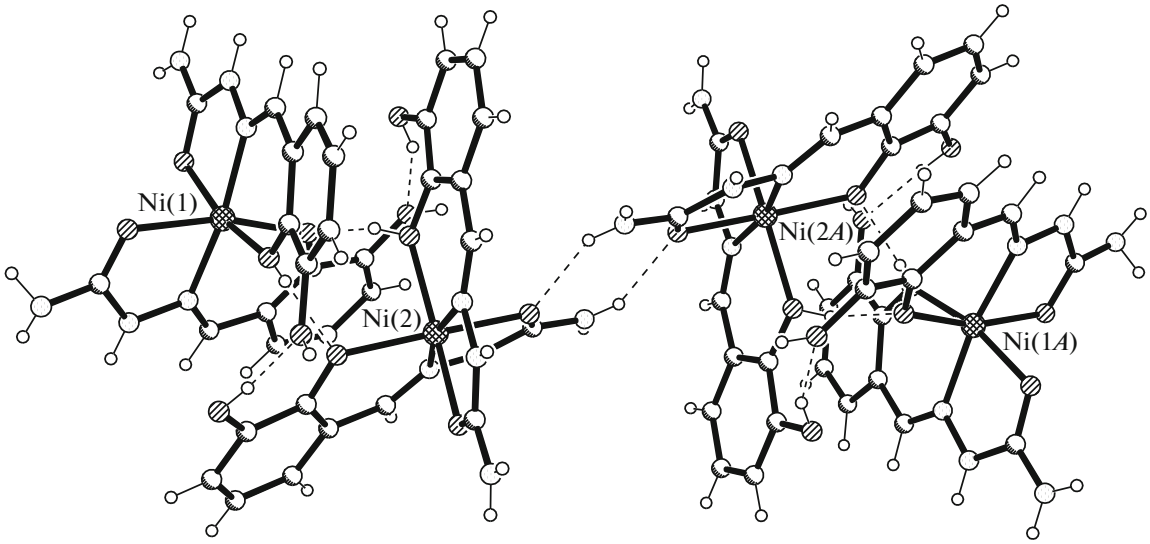

Fig. 5. Formation of chains from the dimers formed by complex cations **A** and **B** in compound **II**.

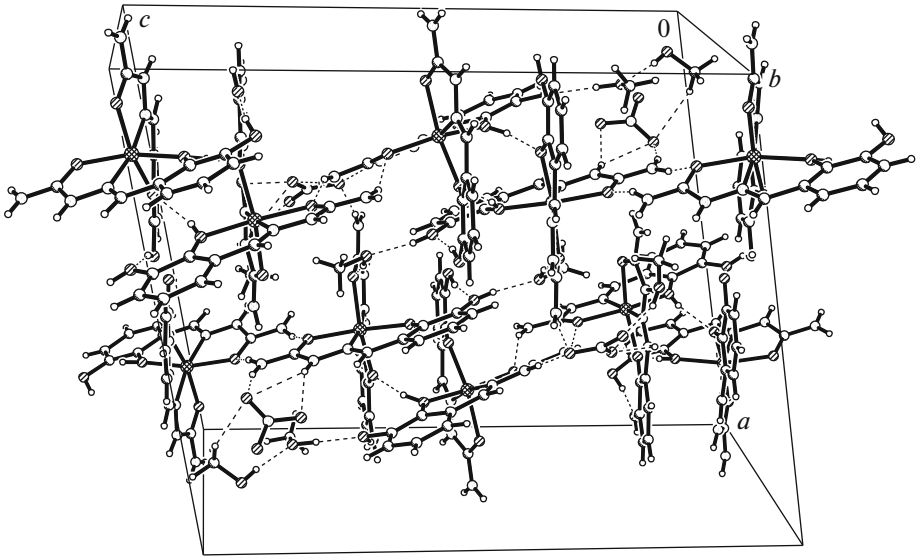

Fig. 6. Packing fragment in compound **II**.

ligand and Cl^- anions as acceptors to form C(2)–H···O(1) (x, $-y + 2$, $z - 1/2$) (C···O 3.179 Å, H···O 2.36 Å, angle CHO 146°) and C–H···Cl ($x - 1/2$, $-y + 3/2$, $z - 1/2$) (C···Cl 3.727 Å, H···Cl 2.92 Å, angle CHO 142°).

The structural studies of the Ni(II) complexes with the semicarbazone derivatives of salicylaldehyde bearing hydroxy and methoxy groups in the meta position in addition to the *ortho*-OH group in the aromatic ring showed that the latter exerted no effect on their coordination mode and they acted as tridentate chelating ligands. During coordination, these ligands are stabilized in both the deprotonated and neutral states to form molecular or ionic complexes involving outer-sphere anions for charge compensation. The presence of nondeprotonated functional groups in the ligands increases the number of hydrogen bonds, which leads to the formation of diverse supramolecular architectures in the crystals.

FUNDING

This work was supported by state programs nos. 20.80009.5007.28, 20.80009.5007.27, 20.80009.5007.04,

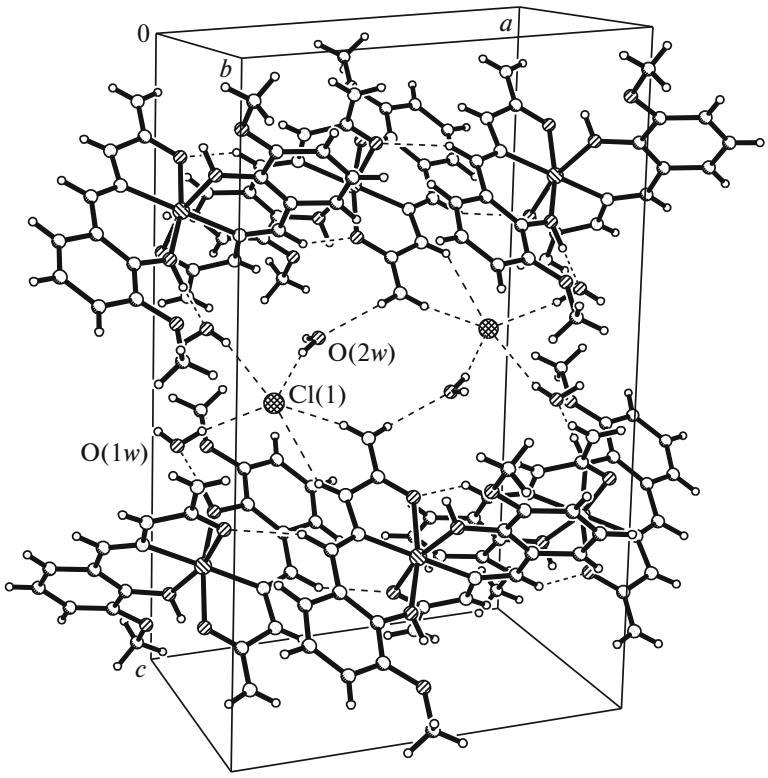

Fig. 7. Packing fragment in compound **III**.

and 20.80009.5007.15 of the National Agency for Research and Development of Moldova.

CONFLICT OF INTEREST

The authors declare that they have no conflicts of interest.

REFERENCES

1. *Supramolecular Chemistry, Concepts and Perspectives*, Lehn, J.-M., Ed., Weinheim: VCH, 1995, p. 271.
2. Balzani, V., Gedi, A., Raymo, F.M., and Stoddart, J.F., *Angew. Chem., Int. Ed.*, 2000, vol. 39, p. 3348.
3. Sadhukhan, D., Ray, A., Pilet, G., et al., *Bull. Chem. Soc. Jpn.*, 2011, vol. 84, no. 7, p. 764.
4. Vrdoljak, V., Pavlovic, G., Hrenar, T., et al., *RSC Adv.*, 2015, vol. 5, p. 104870.
5. Sadhukhan, D., Ghosh, P., Gómez-García, C.J., and Rouzieres, M., *Magnetochem.*, 2018, vol. 4, p. 56.
6. Beraldo, H. and Gambino, D., *Mini-Rev. Med. Chem.*, 2004, vol. 4, p. 31.
7. Dutta, S., Padhye, S., Priyadarsini, K.I., and Newton, C., *Bioorg. Med. Chem. Lett.*, 2005, vol. 15, p. 2738.
8. de Oliveira, R.B., de Souza-Fagundes, E.M., Soares, R.P.P., et al., *Eur. J. Med. Chem.*, 2008, vol. 43, p. 1983.
9. Noblıa, E.J., Baran, L., Otero, P., et al., *Eur. J. Inorg. Chem.*, 2004, no. 2, p. 322.
10. Salem, N.M.H., Rashad, A.R., El Sayed, L., et al., *Inorg. Chim. Acta*, 2015, vol. 432, p. 231.
11. Wang, J.-L., Liu, B., Yang, B.-S., and Huang, S.-P., *J. Struct. Chem.*, 2008, vol. 49, no. 3, p. 570.
12. Wang, J.-L., Feng, J., Xu, M.-P., and Yang, B.-Sh., *Spectrochim. Acta*, 2011, vol. A78, p. 1245.
13. Sadhukhan, D., Ray, A., Pilet, G., et al., *Inorg. Chem.*, 2011, vol. 50, p. 8326.
14. Sutradhar, M., Martins, L.M.D.R.S., Guedes Da Silva, M.F.C., et al., *Dalton Trans.*, 2014, vol. 43, p. 3966.
15. Sadhukhan, D., Maiti, M., Pilet, G., et al., *Eur. J. Inorg. Chem.*, 2015, vol. 2015, no. 11, p. 1958.
16. Ray, A., Rizzoli, C., Pilet, G., et al., *Eur. J. Inorg. Chem.*, 2009, no. 20, p. 2915.
17. Sutradhar, M., Kirillova, M.V., Guedes Da Silva, M.F.C. et al., *Dalton Trans.*, 2013, vol. 42, p. 16578.
18. Chakraborty, J., Thakurta, S., Pilet, G., et al., *Polyhedron*, 2009, vol. 28, p. 819.
19. Gao, Y.-X., Wang, L.-B., and Niu, Y.-L., *Acta Crystallogr., Sect. E: Struct. Rep. Online*, 2007, vol. 63. m2128.
20. Guan, G., Gao, Y., Wang, L., and Wang, T., *Acta Crystallogr., Sect. E: Struct. Rep. Online*, 2007, vol. 63. m2662.
21. Sutradhar, M., Fernandes, A.R., Silva, J., et al., *J. Inorg. Biochem.*, 2016, vol. 155, p. 17.
22. Cuba, L., Bourosh, P., Kravtsov, V., et al., *Chem. J. Moldova. General, Industrial and Ecological Chemistry*, 2018, vol. 13, no. 1, p. 36.

23. Rogolino, D., Bacchi, A., De Luca, L., et al., *J. Biol. Inorg. Chem.*, 2015, vol. 20, p. 1109.
24. Binil, P.S., Anoop, M.R., Suma, S., and Sudarsanakumar, M.R., *J. Therm. Anal. Calorim.*, 2013, vol. 112, no. 2, p. 913.
25. Bovey, F.A., Mirau, P., and Gutowsky, H.S., *Nuclear Magnetic Resonance Spectroscopy*, Academic, 1988, p. 461.
26. *CrysAlis RED. O.D.L. Version 1.171.34.76*, 2003.
27. Sheldrick, G., *Acta Crystallogr., Sect. A: Found Crystallogr.*, 2008, vol. 64, no. 1, p. 112.
28. Sheldrick, G.M., *Acta Crystallogr., Sect. C: Struct. Chem.*, 2015, vol. 71, p. 3.
29. Jayanthi, K., Meena, R.P., Chithra, K., et al., *J. Pharm. Chem. Biol. Sci.*, 2017, vol. 5, no. 3, p. 205.
30. Fernández, M., Becco, L., Correia, I., et al., *J. Inorg. Biochem.*, 2013, vol. 127, p. 150.
31. Valdes-Martinez, J., Toscano, R.A., Salcedo, R., et al., *Monatsh. Chem.*, 1990, vol. 121, p. 641.
32. Naik, D.V. and Palenik, G.J., *Acta Crystallogr., Sect. B: Struct. Crystallogr. Cryst. Chem.*, 1974, vol. 30, p. 2396.
33. Aravindakshan, A.A., Sithambaresan, M., and Prathapachandra Kurup, M.R., *Acta Crystallogr., Sect. E: Struct. Rep. Online*, 2013, vol. 69, p. o586.
34. de Lima, D.F., Perez-Rebolledo, A., Ellena, J., and Beraldo, H., *Acta Crystallogr., Sect. E: Struct. Rep. Online*, 2008, vol. 64, p. o177.
35. Chumakov, Yu.M., Tsapkov, V.I., Byushkin, V.N., et al., *Russ. J. Coord. Chem.*, 1995, vol. 21, no. 12, p. 919.
36. Zirnrner, M., Schulte, G., Luo, X.-L., and Crabtree, R.H., *Angew. Chem., Int. Ed.*, 1991, vol. 2, p. 193.

Translated by E. Yablonskaya